第 30 卷第 8 期
2014 年 8 月

无 机 化 学 学 报
CHINESE JOURNAL OF INORGANIC CHEMISTRY

Vol.30 No.8
1925-1930

2-氨甲基-1*H*-苯并咪唑钴(Ⅱ)和镍(Ⅱ)配合物的合成、晶体结构和抑菌活性

赵海燕*,[1] 马晶军[2] 杨晓东[1] 杨敏丽[1]

([1]河北科技大学理学院,石家庄 050018)

([2]河北农业大学理学院,保定 070001)

摘要:利用双齿配体 2-氨甲基-1*H*-苯并咪唑(AMBI)和硫氰酸钾以及硝酸钴或硝酸镍在甲醇–水中反应制备了 2 个新的异质同晶配合物 *trans*-[M(AMBI)$_2$(NCS)$_2$](**1**:M=Co^{2+},**2**:M=Ni^{2+})。X-射线衍射单晶结构表明:2 个配合物属于单斜晶系,*C*2/*c* 空间群,M(Ⅱ)与来自 AMBI 的 4 个氮原子和异硫氰酸根的 2 个氮原子配位,形成八面体结构。配合物中的 N–H…S 氢键和 π-π 相互作用将配合物连接成三维网络结构。用红外光谱、紫外–可见光谱对配合物 **1** 和配合物 **2** 进行了表征,并对配合物的热稳定性做了研究。选取金黄色葡萄球菌和大肠杆菌作为抑菌菌种,研究了配体 AMBI 和 2 个配合物的抑菌能力。

关键词:钴(Ⅱ)配合物;镍(Ⅱ)配合物;2-氨甲基-1*H*-苯并咪唑;晶体结构;抑菌活性

中图分类号:O614.81^{+}2;O614.81^{+}3 **文献标识码**:A **文章编号**:1001-4861(2014)08-1925-06

DOI:10.11862/CJIC.2014.272

Cobalt(Ⅱ) and Nickel(Ⅱ) Complexes Based on 2-Aminomethyl-1*H*-benzimidazole: Synthesis, Crystal structure and Antibacterial Activity

ZHAO Hai-Yan*,[1] MA Jing-Jun[2] YANG Xiao-Dong[1] YANG Min-Li[1]

([1]*College of Science, Hebei University of Science and Technology, Shijiazhuang* 050018, *China*)

([2]*College of Science, Hebei University of Agriculture, Baoding, Hebei* 070001, *China*)

Abstract: The reaction of M(NO$_3$)$_2$·6H$_2$O with KSCN in presence of the bidentate ligand 2-aminomethyl-1*H*-benzimidazole (AMBI) afforded the six-coordinate mononuclear dithiocyanato-M(Ⅱ) complexes *trans*-[M(AMBI)$_2$(NCS)$_2$] (**1**: M=Co^{2+}, **2**: M=Ni^{2+}). The compounds were characterized by elemental analysis, IR and UV-Vis spectroscopy and their molecular structures were determined by single-crystal X-ray crystallography. In the two complexes, six-coordinate geometry was achieved by the six N-donors of two AMBI and two thiocyanato ligands. Crystal packing of each complex revealed that 3D framework is formed by two hydrogen bonds of type N–H…S and both benzimizazole ring head to tail π-π stacking interactions and face to face π-π stacking interactions. The thermal stability of the complexes was investigated in the solid state. The preliminary antibacterial activities of AMBI and its complexes were investigated as well. CCDC: 936030, **1**; 936031, **2**.

Key words: cobalt(Ⅱ) complex; nickel(Ⅱ) complex; 2-aminomethyl-1*H*-benzimidazole; crystal structure; antibacterial activity

The bidentate ligand 2-aminomethylbenzimidazole (AMBI) has strong coordination ability and can coordinate to metal ions via two nitrogen atoms of the pendant aminomethyl group and the imidazole ring. The amino group and imidazole ring of AMBI are capable of acting as hydrogen bonds donors and the

收稿日期:2013-11-13。收修改稿日期:2014-03-12。

河北科技大学校立基金(No.sw19)资助项目。

*通讯联系人。E-mail:hbhaiyanzh@163.com;会员登记号:S06N6511M1009。

large aromatic system can provide potential supramolecular recognition sites for π-π stacking interactions that can be used to govern the process of self-assembly[1-5]. On the other hand, since Roderick[6] and his coworkers firstly reported that bisbenzimidazoles were potent inhibitors of rhinoviruses in 1972, the study of the bisbenzimidazolyl complexes has increasingly caught researchers′ eyes[7-9]. Attributed to their special physiological activities, some bisbenzimidazolyl complexes have been investigated and even applied in medicine to prevent or cure some diseases[10-11]. SCN^- is a linear ligand with two donor atoms and may coordinate through terminal modes or bridging modes or both, with great potential in building a coordination network[12-15]. The Cu(Ⅱ)-AMBI/SCN^- has been synthesized; it is the only example of a structurally characterized AMBI/SCN^--transition metal complex[14]. Accordingly, AMBI was used as the main ligand and SCN^- as auxiliary ligand for the synthesis of Co(Ⅱ) and Ni(Ⅱ) complexes in this work. Herein, we report the syntheses and structural characterization of $[Co(AMBI)_2(NCS)_2]$ (**1**) and $[Ni(AMBI)_2(NCS)_2]$ (**2**), whose preliminary biological tests have been explored.

1 Experimental

1.1 Materials and physical measurements

The ligand AMBI was prepared following a published procedure[16-17]. All solvents and reagents were of commercially analytical grade and used without further purification. Elemental analyses for C, H and N were taken by using a Model 240 Perkin-Elmer elemental analyzer. The infrared spectrum was obtained on a ThermoFisher Nicolet 6700 spectrometer with KBr pellets in the 4 000~400 cm^{-1} region. A Shimadzu UV-2550 spectrophotometer was used to record the electronic spectra. Thermogravimetric analysis was obtained using a SDT Q600 V20.9 Build 20 TG-DTA/DSC instrument at a heating rate of 5 ℃·min^{-1} under an air atmosphere.

1.2 Synthesis of coumpouds

1.2.1 Synthesis of $[Co(AMBI)_2(NCS)_2]$ (**1**)

A methanol solution (5 mL) of $Co(NO_3)_2·6H_2O$ (0.1 mmol, 29.1 mg) was mixed with AMBI (0.2 mmol, 29.4 mg) dissolved in 10 mL methanol solution. To the resulting solution was added 5 mL methanol solution of KSCN (0.2 mmol, 19.4 mg) with stirring. The pink solution was allowed to slowly evaporate into a beaker covered with plastic paper. Pink crystals suitable for X-ray studies were formed in several days Anal. Calcd. for $C_{18}H_{18}CoN_8S_2$ (%): C, 46.05; H, 3.86; N, 23.87. Found (%): C, 46.08; H, 3.92, N, 23.81. IR (cm^{-1}, KBr), 3 345m, 3 251m, 3 230m, 2 100s, 1 625w, 1 452m, 1 023m.

1.2.2 Synthesis of $[Ni(AMBI)_2(NCS)_2]$ (**2**)

The analogous reaction of $Ni(NO_3)_2·6H_2O$ with AMBI produced blue-purple prism crystals of **2**. Anal. Calcd. for $C_{18}H_{18}NiN_8S_2$ (%): C, 46.08; H, 3.87, N, 23.87. Found (%): C, 46.12; H, 3.85, N, 23.84. IR (cm^{-1}, KBr), 3 344m, 3 253m, 3 223m, 2 100s, 1 609 w, 1 453m, 1 023m.

1.3 Crystal structure determination

The diffraction data for complexes **1** and **2** were collected on a Bruker Smart APEX Ⅱ CCD diffractometer equipped with graphite-monochromated Mo $K\alpha$ radiation (λ=0.071 073 nm). The structures were solved by direct methods and refined by full-matrix least-squares on F^2 using the SHELXTL program package[18]. All nonhydrogen atoms were refined anisotropically. Hydrogen atoms were generated geometrically and refined as riding models. Table 1 lists the crystal data and structure refinement parameters for complexes **1** and **2**. Table 2 summarized selected bond lengths and angles for complexes **1** and **2**.

CCDC: 936030, **1**; 936031, **2**.

1.4 Biological activity tests

Complex **1** and **2** were tested *in vitro* to assess its growth inhibitory activity against one Gram positive bacteria, viz. *Staphylococcus aureus* one Gram negative bacteria viz. *Escherichia coli* by the disk diffusion method[10]. The antibacterial activities of AMBI were also evaluated during the same experiment. The bacterial strains grown on nutrient agar at 37 ℃ for 18 h were suspended in a saline solution (0.85% NaCl) and adjusted to a turbidity of 0.5 MacFarland standards (10^8 CFU·mL^{-1}). The suspension was used to inoculate sterile Petri plates of 9.0 cm diameter in

Table 1　Crystallographic data and refinement summary for the complexes 1 and 2

Complex	**1**	**2**
Formula	$C_{18}H_{18}CoN_8S_2$	$C_{18}H_{18}NiN_8S_2$
Formula weight	469.47	469.23
Crystal system	Monoclinic	Monoclinic
Space group	*C*2/*c*	*C*2/*c*
a / nm	1.553 95(19)	1.542 25(10)
b / nm	0.827 38(11)	0.829 22(6)
c / nm	1.65 14(2)	1.652 28(8)
β / (°)	108.465(2)	108.997(2)
V / nm^3	2 014.0(4)	1 998.0(2)
Z	4	4
D_c / (g·cm^{-3})	1.548	1.560
Crystal size / mm	0.30×0.30×0.20	0.40×0.32×0.30
F(000)	964	968
Reflections collected	4 873	3 561
Reflections unique (R_{int})	1 777 (0.023 6)	1 762 (0.027 6)
Observed reflections ($I \geqslant 2\sigma(I)$)	1 672	1 449
R_1, wR_2 ($I \geqslant 2\sigma(I)$)	0.031 2, 0.084 4	0.033 3, 0.066 6
R_1, wR_2 (all data)	0.032 8, 0.085 3	0.046 5, 0.073 2
Goodness-of-fit on F^2	1.093	1.042
Max. res peak and hole / (e·nm^{-3})	641, −354	231, −281

Table 2　Selected bond distances (nm) and angles (°) for complex 1 and 2

Complex **1**					
Co1-N1	0.209 55(15)	Co1-N1A	0.209 55(15)	Co1-N2	0.221 45(14)
Co1-N2A	0.221 45(14)	Co1-N4	0.214 20(13)	Co1-N4A	0.214 20(13)
S1-C1	0.164 6(2)	N1-C1	0.115 2(3)		
N1-Co1-N1A	93.91(9)	N1-Co1-N4A	95.39(5)	N1-Co1-N2A	172.20(6)
N1-Co1-N4	89.88(6)	N1-Co1-N2	87.24(6)	N4A-Co1-N4	172.27(7)
N2A-Co1-N2	92.67(8)	N4-Co1-N2A	97.69(5)	N1-C1-S1	179.18(19)
N4-Co1-N2	76.89(5)	C1-N1-Co1	170.77(17)		
Complex **2**					
Ni1-N1	0.209 4(2)	Ni1-N1A	0.209 4(2)	Ni-N3	0.214 8(2)
Ni1-N3A	0.214 8(2)	Ni1-N4	0.206 9(2)	Ni1-N4A	0.206 9(2)
C9-S1	0.164 4(3)	C9-N3	0.115 3(3)		
N1-Ni1-N1A	173.21(12)	N4-Ni1-N1	89.59(8)	N1-Ni1-N3	79.04(8)
N4-Ni1-N3	87.65(9)	N1-Ni1-N3A	96.23(8)	N4-Ni1-N3A	174.17(9)
N3-Ni1-N3A	93.06(12)	N4A-Ni1-N4	92.24(13)	N4-Ni1-N1A	95.13(8)
C9-N4-Ni1	171.4(2)	N4-C9-S1	179.3(3)		

Symmetry code: complex **1**: A: −*x*, *y*, −*z*+1.5; complex **2**: A: −*x*+1, *y*, −*z*+0.5.

which the test organisms were grown. After solidification, a hole of diameter of 0.6 cm was pierced by a sterile cork borer. **1**, **2** and AMBI were dissolved in dimethylsulfoxide (DMSO) to prepare three different concentrations (125, 250 and 500 μg·mL^{-1}) for evaluation of dose response. The discs were

placed on the holes of previously seeded plates and incubated at 310 K for 24 h. Antibacterial activities of the compounds were evaluated by measuring the inhibition zone diameters (IZD). Each of the above experiments was repeated thrice along with a control set using DMSO and the mean value was taken for comparison.

2 Results and discussion

2.1 Characterization

The IR spectra of the two complexes were analyzed in comparison with that of the free molecule, AMBI, in the region 4 000~400 cm^{-1}. The IR spectrum of the free ligand shows one medium and broad absorption band in the region 3 411~3 280 cm^{-1}, which are stretching vibrations of the -NH- and -NH_2 groups. Both complexes show one medium and broad absorption band in the region 3 344~3 223 cm^{-1}. The red shift in the absorption bands of the complexes are positive signs for complexation of the metals to the amino group of the ligand[19].

Another region of the IR spectra with characteristic changes due to complexation is the 1 700~1 400 cm^{-1}. The free ligand shows one medium absorption band at 1 624 cm^{-1} that is due to the stretching vibration of the C=N group of the imidazole ring. Complex **1** shows one weak absorption band at 1 625 cm^{-1} and complex **2** at 1 609 cm^{-1}. Also, the free ligand shows one medium absorption at 1 442 cm^{-1} that is due to the stretching vibration of C=N-C=C of the benzimidazole. In comparison, absorptions of C=N-C=C of the benzimidazole in complex **1** and complex **2** are at 1 452 and 1 453 cm^{-1}, respectively. Those absorption bands are positive indications for complexation of metals with the benzimidazole group[20].

The appearance of a single ν(CN) band at 2 100 cm^{-1} in the IR spectra of the two complexes indicates that the isothiocyanate groups are probably *cis* coordinated in both complexes excluding the possibility of geometrical isomerism[21]. It has been noted that the ν(CS) frequency of 780~860 cm^{-1} is indicative of N-bonding, while a frequency of 690~720 cm^{-1} indicates S-bonded of thiocyanate group. The medium peaks due to ν(CS) at 854 cm^{-1} and δ(NCS) at 479 cm^{-1} in the IR spectra of the two complexes, occur in the range observed for N-bonded NCS^- moieties in other isothiocyanatochromium(Ⅲ) complexes[22]. Its identity was finally confirmed by X-ray crystallography.

The UV-Vis absorption spectra of AMBI, complex **1** and **2** were determined in MeOH solution. Their absorption bands in the region of 218~280 nm can be assigned to π-π* transitions of the conjugated system. The electronic spectra of $[Co(AMBI)_2(NCS)_2]$ show two strong bands with maximum at approximately 470 and 520 nm, as well as a very weak band at approximately 630 nm. The band at 470 and 520 nm are assigned to the $^4T_{1g}(F)\rightarrow{}^4T_{1g}(P)$ (v_3) and $^4T_{1g}(F)\rightarrow{}^4A_{2g}(v_2)$ transitions, respectively. The very weak band over 630 nm is likely to be the spinforbidden $^4T_{1g}(F)\rightarrow{}^4A_{2g}(G)$ transition[23]. The electronic spectra of $[Ni(AMBI)_2(NCS)_2]$ show two bands with maximum at approximately 390 and 610 nm. These bands are attributable to the $^3A_{2g}\rightarrow{}^3T_{1g}$ (P) and $^3A_{2g}\rightarrow{}^3T_{1g}$ transitions, respectively, and indicate of octahedral Ni(Ⅱ) compounds.

2.2 Crystal structures of the complexes

Fig.1 gives the crystal structure of complex **1** with atomic labeling scheme.

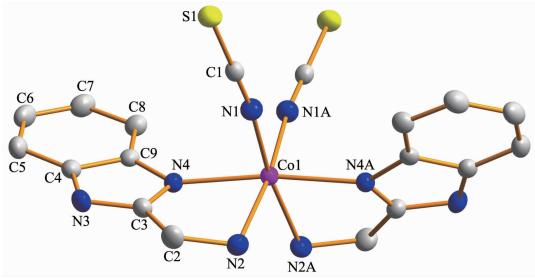

Symmetry code: A $-x$, y, $-z+1.5$

Fig.1 Crystal structure of complex **1** with atomic labeling scheme and 30% thermal llipsoids

Single-crystal X-ray diffraction studies revealed that the new complexes **1** and **2** are isomorphous, so only the structure of **1** is described in detail here. In complex **1** the Co(Ⅱ) coordination is distorted-octahedral with the four N-atoms of two AMBI ligands and two N-atoms of two isothiocyanate groups. The Co-N(imidazole) and Co-N(amine) bond distances are 0.214 20(13) nm and 0.221 45(14) nm, respectively. It is noteworthy that the Co-N (imidazole) bond

distancese are shorter than the Co-N (amine) bond distances. This difference can be explained by availability of a favorable back-bonding of electron density from the Co center into the imidazole N=C π^* orbital[24]. Two thiocyanate groups coordinate to the metal ion as terminal ligands in trans positions. The Co-N(thiocyanate) distance is 0.209 55(15) nm. The thiocyanate groups almost linear with the N-C-S bond angle of 179.18(19)°. The Ni-N-C bond angles are 170.77(17)°, deviating from 180° expected for the *sp* hybrid orbital of the N atom. The C-N distance of 0.115 2(3) nm and C-S of 0.164 6(2) nm in the SCN- moiety show the normal structure of the thiocyanate in the complex.

The crystal structure of the complex **1** can be described as a 3D network due to two types of intermolecular hydrogen bonds and π-π stacking interactions. Atom S1 of the terminal thiocyanate ligand interacts with H2D of the pendant aminomethyl group of the neighboring complex with H2D⋯S1^{i} and N2 ⋯ S1^{i} diastances of 0.264 9 and 0.352 7 nm, respectively (symmetry code: ^{i} $-x+0.5$, $-0.5+y$, $-z+1.5$). Again atom S1 exhibits a hydrogen bonding interaction with H3A attached to the benzimidazole N atom of an adjacent complex with H2D⋯S1^{ii} and N3 ⋯ S1^{ii} diastances of 0.259 3 nm and 0.336 6 nm, respectively (symmetry code: ^{ii} $-x+0.5$, $-y+0.5$, $-z+2$). The two types of N–H ⋯ S hydrogen bonds extend complex 1 into a 2D layers parallel to the *ac* plane (Fig.2). In addition to this an interesting feature in the packing diagrams of complex **1** is that both types of aromatic π-π stacking interactions are observed (Fig. 3). One type is the head to head π-π stacking interacions from benzimidazole rings. The adjacent benzimidazole rings (benzene ring is designated as ring 1 with centroid Cg1 and corresponding imidazole ring as ring 2 with centroid Cg2) involved in the π-π sacking interactions. The perpendicular distance from Cg1 to the plane of symmetry-related ring 2, and from Cg2 to the plane of symmetry-related ring 1 are 0.362 57 and 0.362 50 nm, respectively. The distance between the ring centroids (Cg1⋯Cg2) are 0.377 7 and 0.381 9 nm, respectively. The other type is the head to tail π-π stacking interactions from benzimidazole rings. The distances of neighboring parallel benzene rings are 0.342 85 nm, with a center-to-center separation of 0.372 2 nm. These π-π stacking interactions play vital roles in stabilizing the entire 3D supramolecular structure.

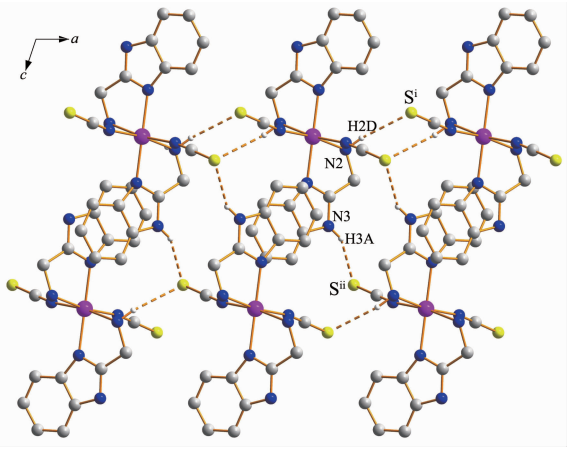

Symmetry codes: ^{i} $-x+0.5$, $-0.5+y$, $-z+1.5$; ^{ii} $-x+0.5$, $-y+0.5$, $-z+2$

Fig.2　2D network in complex **1** parallel to the *ac* plane

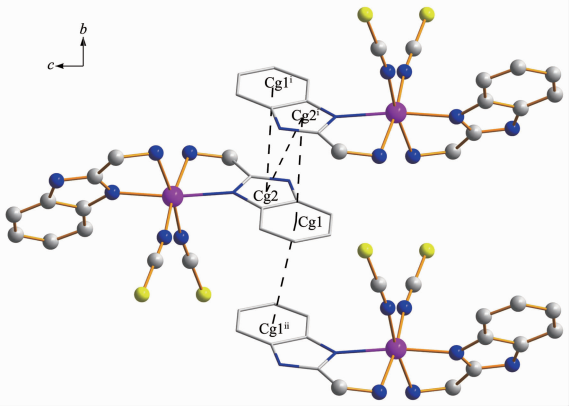

Symmetry codes: ^{i} $-x$, $-y$, $-z+2$; ^{ii} $-x$, $-y+1$, $-z+2$

Fig.3　View of $\pi\cdots\pi$ interactions between benzimidazole rings

2.3　Thermogravimetric (TG) analyses

Thermogravimetric experiments were conducted to study the thermal stability of complexes **1** and **2**, which is an important parameter of inorganic-organic hybrid materials. The TG properties of complexes **1** and **2** were measured under air atmosphere from 18 to 800 ℃. For **1**, the first weight loss of 30.81% in the range of 250~438 ℃ corresponds to the loss of one benzimizazole ring and one CH_2 group (Calcd. 28.15%). After 438 ℃, the residue starts to decompose.

For complex **2**, the weight loss of 25.63% from 267 to 340 ℃ is attributed to the loss of one benzimizazole ring (Calcd. 25.17%). There is no further weight loss from 340 to 419 ℃. After that temperature, the residue starts to decompose.

2.4 Antibacterial activity of the compounds

The antibacterial activities of all of the tested compounds as IZD are presented in Table 5. The IZD data show that **1** and **2** are active against *S. aureus* and *E. coli* whereas AMBI is active against *S. aureus* but is inactive against *E. coli*. From the *in vitro* antibacterial assay, it is observed that the tested compounds possess mild to moderate antibacterial activities which increase with dose. The complexes have stronger antibacterial activities against *S. aureus* than the free AMBI ligand. It is obvious that **2** has stronger activities against *E. coli* than **1**.

Table 5 Antibacterial activities of 1, 2 and AMBI

Compounds	Dose / ($\mu g \cdot mL^{-1}$)	Inhibition zone diameter in mm	
		S. aureus	*E. coli*
AMBI	125	—	—
	250	16	—
	500	19	—
1	125	18	—
	250	18	11
	500	21	15
2	125	—	—
	250	18	17
	500	21	21
DMSO	AR	—	—

Reference:

[1] Jordi G S, María J P, Mercè F B, et al. *Inorg. Chem.*, **2006**, **45**:10031-10033

[2] Liu H Y, Wu H, Ma J F, et al. *Cryst. Growth Des.*, **2010**,**10**: 4795-4805

[3] Peng G, Qiu Y C, Liu Z H, et al. *Cryst. Growth Des.*, **2010**, **10**:114-121

[4] Yang X P, Jone R A, Wiester M J, et al. *Cryst. Growth Des.*, **2010**,**10**:970-976

[5] Wang C J, Yue K F, Tu Z X, et al. *Cryst. Growth Des.*, **2011**,**11**:2897-2904

[6] Roderick W R, Nordeen C W, Von Esch A M, et al. *J. Med. Chem.*, **1972**,**15**:655-658

[7] Yeung K S, Meanwell N A, Qiu Z, et al. *Bioorg. Med. Chem. Lett.*, **2001**,**11**:2355-2359

[9] Tong L. *Chem. Rev.*, **2002**,**102**:4609-4625

[9] Lootiens F G, Regenfuss P, Zechel A, et al. *Biochemistry*, **1990**,**29**:9029-9039

[10]Geratz J D, Tidwell R R, Lombardy R J, et al. *Am. J. Pathol.*, **1991**,**139**:921-931

[11]Tebbe M J, Spitzer W A, Victor F. *J. Med. Chem.*, **1997**,**40**: 3937-3946

[12]Rahaman S H, Ghosh R, Mostafa G, et al. *Inorg. Chem. Commun.*, **2005**,**8**:700-703

[13]Silva da P B, Frem R C G, Netto A V G, et al. *Inorg. Chem. Commun.*, **2006**,**9**:235-238

[14]Jiang Y B, Kou H Z, Gao F, et al. *Acta Cryst.*, **2004**,**C60**: m261-m262

[15]Bai Y, Gou H, Dang D B, et al. *J. Mol. Struct.*, **2009**,**934**: 53-56

[16]Lawrence A C, Alan R D. *J. Org. Chem.*, **1962**,**27**:581-586

[17]Gök Y, Karaböcek S, Msr M N. *Transition Met. Chem.*, **1998**,**23**:333-336

[18]Sheldrick G M. *SHELXL*-97, *Program for X-ray Crystal Structure Solution*, Göttingen University, Germany, **1997**.

[19]Mylonas S, Valavanidis A, Dimitropoulos K, et al. *J. Inorg. Biochem.*, **1998**,**34**:265-275

[20]Lord R C, Thomas G J. *Spectrochim. Acta, A*, **1967**,**23**:2551 -2591

[21]Laskar I R, Maji T K, Chaudhuri S, et al. *Polyhedron*, **2000**, **19**:1803-1807

[22]Choi J H, Lee S H. *J. Mol. Struct.*, **2009**,**932**:84-89

[23]Eilbeck W J, Holmes F, Underhill A E. *J. Chem. Soc. A*, **1967**:757-761

[24]Luo H, Lo J M, Fanwick P E, et al. *Inorg. Chem.*, **1999**,**38**: 2071-2078